

Physics of Two-Dimensional Ferroelectric Polymers

Stephen Ducharme

*Department of Physics and Astronomy
Center for Materials Research and Analysis
University of Nebraska, Lincoln, NE 68588-0111, USA
sducharme1@unl.edu*

S. P. Palto, L. M. Blinov, and V. M. Fridkin

*Institute of Crystallography, Russian Academy of Sciences, 11733 Moscow, RUSSIA
fridkin@ns.crys.ras.ru*

Abstract. Unique insight into the nature of ferroelectricity is emerging from the study of Langmuir-Blodgett films of vinylidene fluoride copolymers. These films are the first truly two-dimensional ferroelectrics, with thickness-independent bulk ferroelectric properties and a separate surface phase transition.

FERROELECTRIC POLYMERS

The Teflon™-like polymer polyvinylidene fluoride (PVDF) and its copolymers with trifluoroethylene, and tetrafluoroethylene are a rich system for the study of ferroelectricity,¹⁻³ while the rapid commercialization of piezoelectric transducers made from these materials is a model of technology transfer.⁴

Though crystalline ferroelectric polymers were discovered over thirty years ago, the samples made by solvent casting and spin coating methods were polymorphous, containing multiple phases and incompletely oriented crystallites.⁴ Perhaps the best recent examples of solvent-formed ferroelectric polymers are films formed by spinning on textured Teflon⁵ or by combined casting and stretching and poling.⁶ Though much has been learned about the fundamental nature of ferroelectricity and related properties of PVDF copolymers, the polymorphous films limit the detail and accuracy of experiments and many questions remained unanswered.

The C₂H₂F₂ molecular units in the polymer chains of PVDF have net dipole moments, pointing from the relatively electronegative fluorine to the hydrogen and can crystallize in an arrangement with macroscopic polarization. Figure 1a shows the all-trans (*TTTT*) conformation of the polar β phase, which crystallizes in a quasihexagonal polar packing as shown in Fig. 1c. Another important crystal phase is composed of the alternating trans-gauche (*TGTG*) conformation shown in Fig. 1b, which packs with no net polarization in the paraelectric α phase as in Fig. 1d.

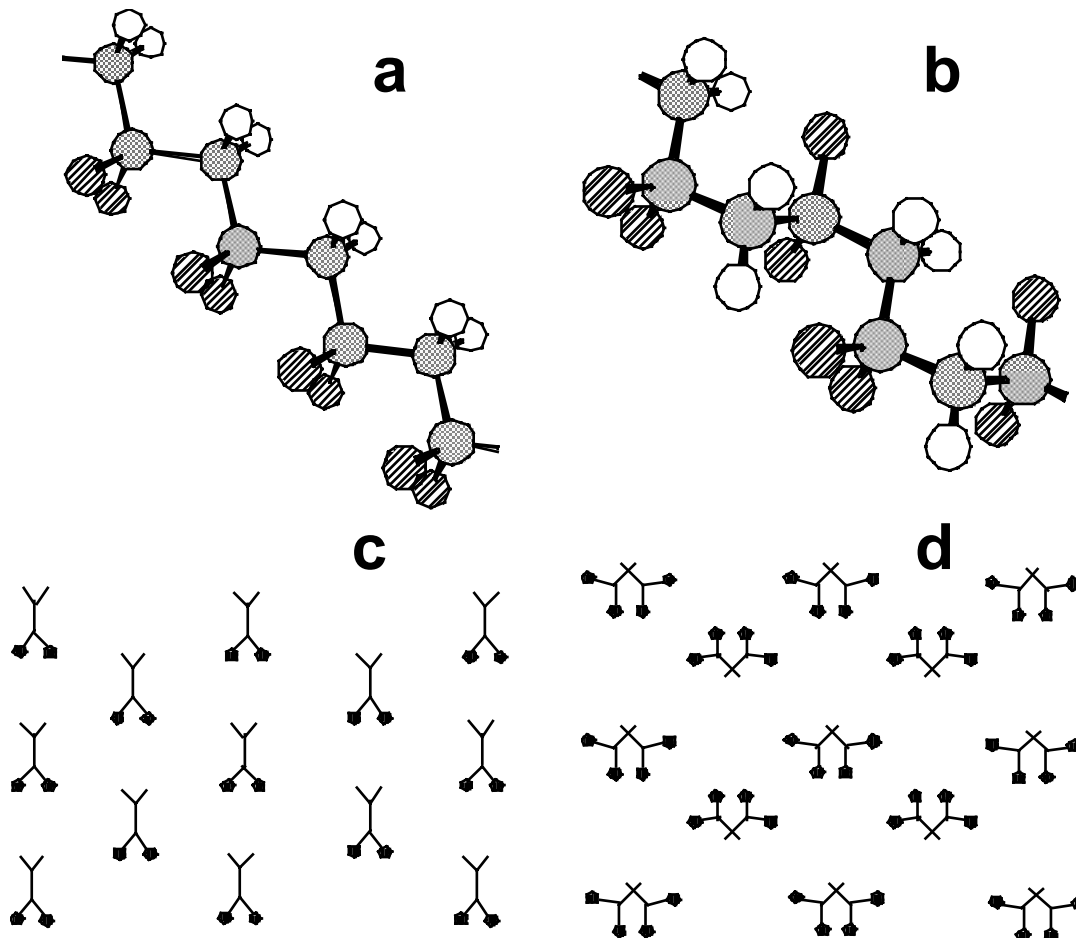


FIGURE 1. Structure of PVDF; carbons are gray, fluorines striped, hydrogen white: a) All-trans *TTTT* conformation of the ferroelectric β phase; b) Alternating trans-gauche *TGTG* conformation of the paraelectric α phase; c) Crystal structure of the β phase; d) Crystal structure of the α phase.

LANGMUIR-BLODGETT FILMS OF PVDF COPOLYMERS

Fabrication

In 1995 we began studies of ultrathin ferroelectric Langmuir-Blodgett (LB) films of PVDF and its copolymers with trifluoroethylene, P(VDF-TrFE).⁷ The films are fabricated one monolayer (ML) at a time by repeatedly dipping a substrate into a liquid subphase coated with a monolayer of the desired polymer.⁸ Most films are produced by horizontal (Schaefer) dipping as shown in the inset of Fig. 2a, but vertical dipping also makes excellent films. Films are deposited at room temperature at a surface pressure of 5 mN/m or less, to prevent collapse, as indicated by the two-dimensional pressure-area diagram in Fig. 2a. Films of thickness 1-500 ML have been made on a variety of substrates with and without metal electrodes. Unless otherwise noted the completed samples were constructed as follows: films for structure measurements were deposited on silicon wafers without any metal electrodes; films

for dielectric measurements were deposited on glass with evaporated aluminum electrodes top and bottom of the films.

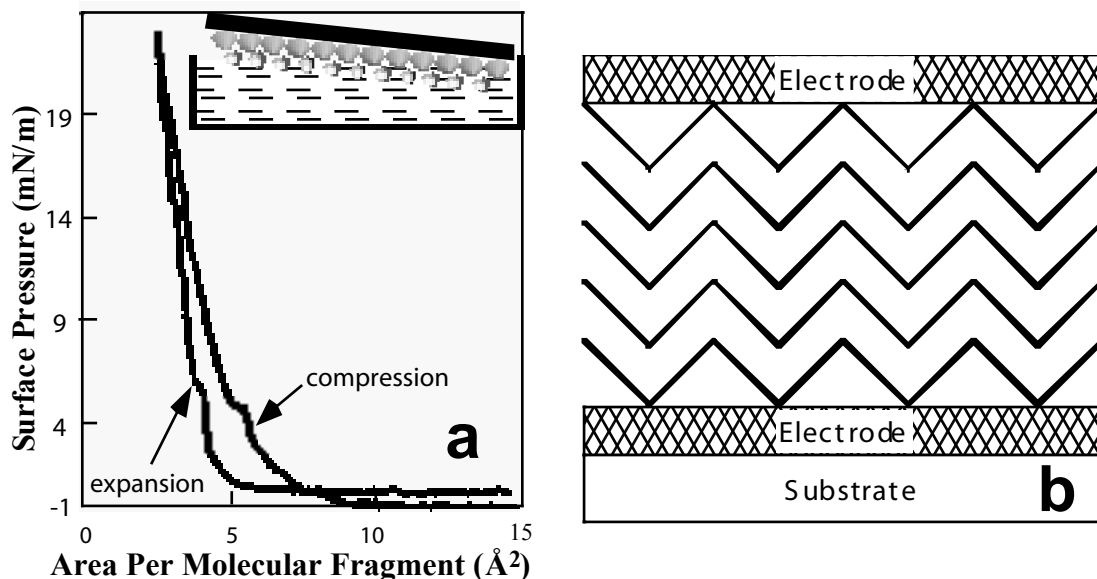


FIGURE 2. a) Surface pressure of a Langmuir monolayer on the water surface. (Adapted from Ref. 7, © 1995 Overseas Publishers Association, N.V., reprinted with permission from Gordon and Breach Publishers.) Inset: horizontal transfer technique; b) Sample construction.

Structure

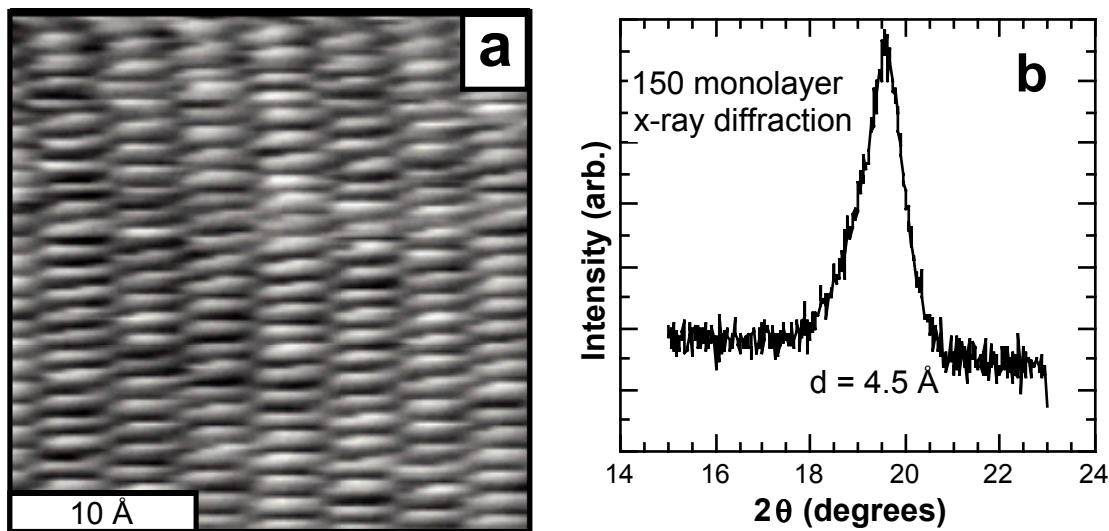


FIGURE 3. Structure of P(VDF-TrFE 70:30) copolymer LB films: a) STM image with chains running vertically; b) x-ray diffraction from the interlayer spacing in the theta-two-theta geometry.

The LB deposition method produces films with excellent order, as shown in the Scanning Tunneling Microscopy (STM) image in Fig. 3a, while low-energy electron diffraction (LEED) confirms the excellent local crystallinity and the global in-plane orientation of the polymer chains over areas of several square millimeters.⁹ The good bulk crystallinity is confirmed by X-ray diffraction (Fig. 3b)¹⁰ and by neutron

diffraction.¹¹ Scanning Electron Microscopy (SEM) and Atomic Force Microscopy (AFM) show excellent planar morphology of the films over 95 % of their area.

BASIC FERROELECTRIC PROPERTIES

The nm-thickness and high quality of the LB films have helped us achieve what others could not in nearly thirty years of study of ferroelectric polymers. The main results concerning the fundamental nature of ferroelectricity include: the discovery of **two-dimensional ferroelectricity**,¹² the discovery of a new **surface ferroelectric phase transition**,^{12,13} demonstration of double hysteresis and the **ferroelectric critical point** for the first time in a polymer,¹⁴ and the first direct measurement of the **intrinsic ferroelectric coercive field** in any ferroelectric.¹⁵

Ferroelectric-Paraelectric Phase Transition

The films exhibit key features of the first-order ferroelectric-paraelectric phase transition. One feature is the metastability of phases near the transition temperature T_c , which results in thermal hysteresis of film properties. The dielectric response (Fig. 4a) exhibits peaks signifying the change of phase at different temperatures on heating and on cooling. X-ray diffraction measurements of the layer spacing (Fig. 4b) demonstrates this thermal hysteresis and the coexistence of phases in a range of temperatures about T_c .¹⁰

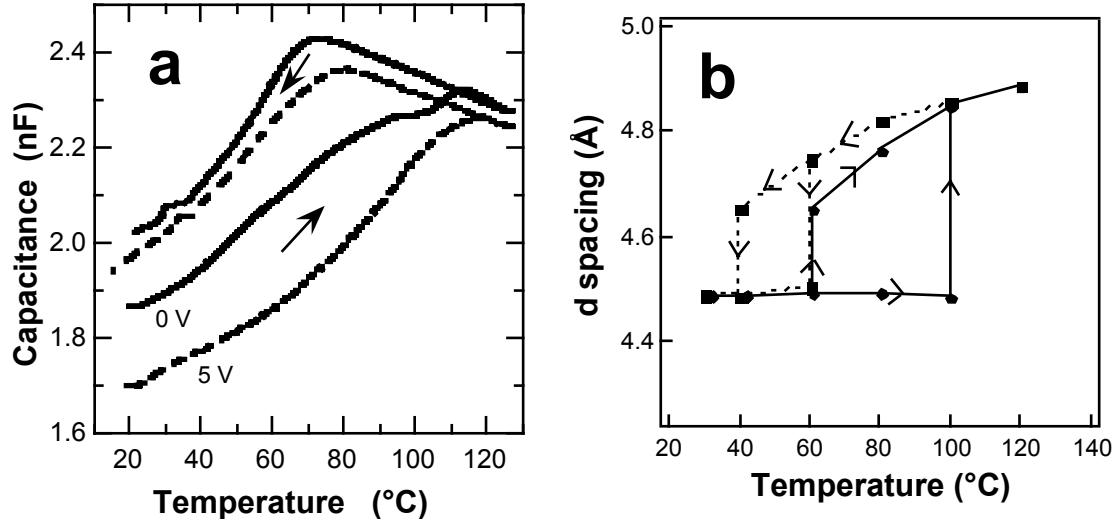


FIGURE 4. Thermal hysteresis at the ferroelectric-paraelectric phase transition: a) The dielectric anomalies at zero electric field and with a field applied (Adapted from Ref.14); b) Layer spacing from X-ray diffraction. (Adapted from Ref. 10.)

Critical Point

The first-order ferroelectric phase transition can be raised by the application of an external electric field, causing reentrant ferroelectricity and double hysteresis, up to a

critical point (T_{cr}, E_{cr}) .¹⁴ The shift in T_c is apparent in the dashed curve of Fig. 4a; application of the field raises the transition temperature on both heating and cooling. Polarization hysteresis is manifest in the 'butterfly' curves, dielectric peaks as the bias voltage is cycled slowly through hysteresis (Fig. 5a). The butterfly curve at 70 °C reveals ordinary single hysteresis below T_c , while above T_c , double hysteresis appears as shown by the four peaks at 90 °C. Above the critical temperature, hysteresis disappears and the butterfly curve closes up as at 150 °C. These results are summarized in the $E - T$ phase diagram (Fig. 5b) constructed from these measurements.¹⁴ X-ray diffraction measurements confirm that the applied field converts the paraelectric α -phase structure to the ferroelectric β -phase structure.

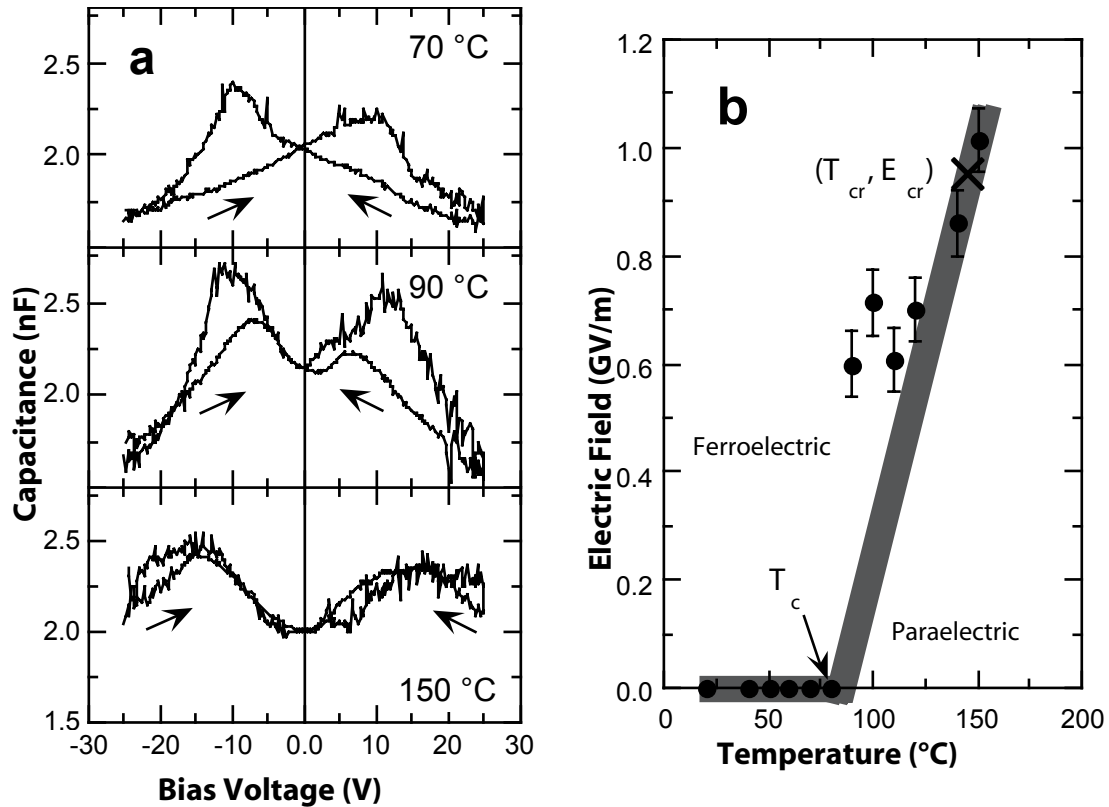


FIGURE 5. a) Butterfly curves showing single hysteresis, double hysteresis, and no hysteresis; b) Phase diagram showing the zero-field phase transition temperature T_c and the critical point (T_{cr}, E_{cr}) . The sample was 30 ML thick. (Adapted from Ref. 14.)

Intrinsic Coercive Field

Normally, the measured coercive field is much lower than the intrinsic value calculated from ferroelectric theory because defects nucleate local polarization reversal at fields below the intrinsic coercive field. But nucleation can be inhibited when sample dimensions are smaller than the minimum nucleation volume. This appears to be the case in the PVDF copolymer LB films with thickness 15 nm or less, where the magnitude of the coercive field fits the Landau-Ginzburg model quantitatively and has the correct dependence on applied field (Fig. 6a) temperature

(Fig. 6b) and sample thickness (Fig. 7b).¹⁵ The coercive field decreases as the sample thickness increases above 15 nm (Fig. 7b), indicating the onset of nucleation.

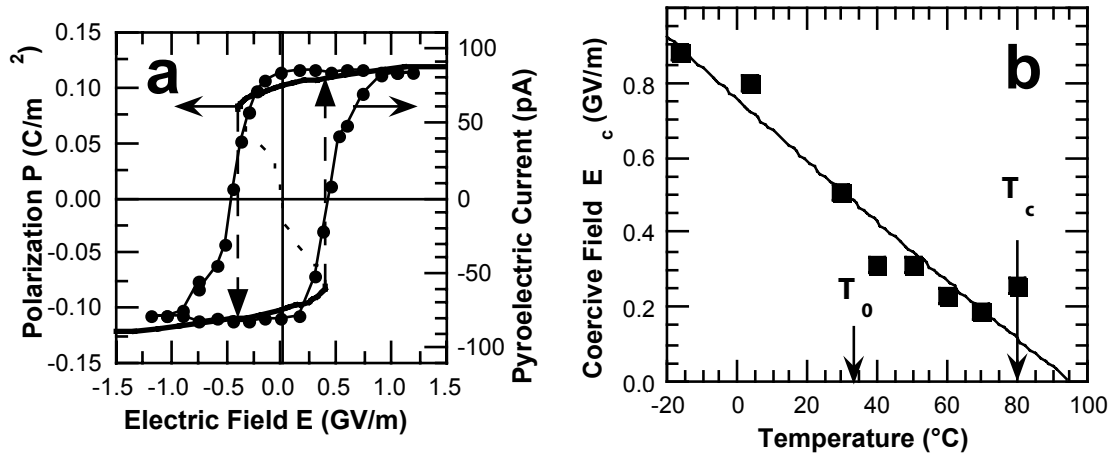


FIGURE 6. The intrinsic coercive field of a 30 ML LB film of P(VDF-TrFE 70:30). (Adapted from Ref. 15.) a) Measured polarization hysteresis at 25 °C overlaid with the intrinsic P - E function; b) Dependence of the coercive field E_c on temperature.

TWO-DIMENSIONAL FERROELECTRICITY

The lack of finite size effects in the LB films thinner than 15 nm proves that P(VDF-TrFE) is essentially a two-dimensional ferroelectric, the first example found.^{12,16} The ferroelectric phase transition temperature is nearly independent of thickness (Fig. 7a) and the intrinsic coercive field is constant below 15 nm thickness. There is no sign of a minimum critical thickness or suppression of the ferroelectric phase that might result from surface and depolarization energies expected for three-dimensional ferroelectricity,¹⁷ and observed in other ferroelectrics.¹⁸⁻²⁰

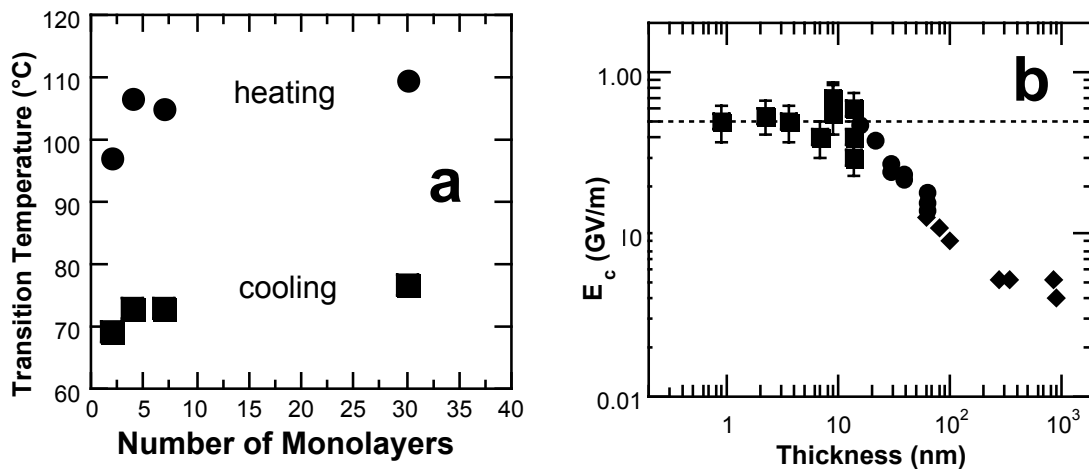


FIGURE 7. Finite-size scaling: a) The dependence of the transition temperature on thickness; b) The coercive field E_c for spun films²¹ (triangles), thick LB films²² (circles) and thin LB films¹⁵ (squares). (Adapted from Ref. 15.)

Surface Phase Transition

We discovered a distinct surface transition near 20 °C (Fig. 8a), well below the 80 °C bulk transition in the thinnest LB films of PVDF and P(VDF-TrFE).¹² The surface phase transition is accompanied by a doubling of the Brillouin zone, as verified by angle-resolved inverse photoemission spectroscopy.^{9,10} This doubling is a result of the conversion of the all-trans chain conformation (Fig. 8b) to the alternating trans-gauche conformation that has been shown to occur at the bulk phase transition. Surface-sensitive second harmonic generation has also confirmed the presence of the surface phase transition in P(VDF-TrFE) LB films.²³

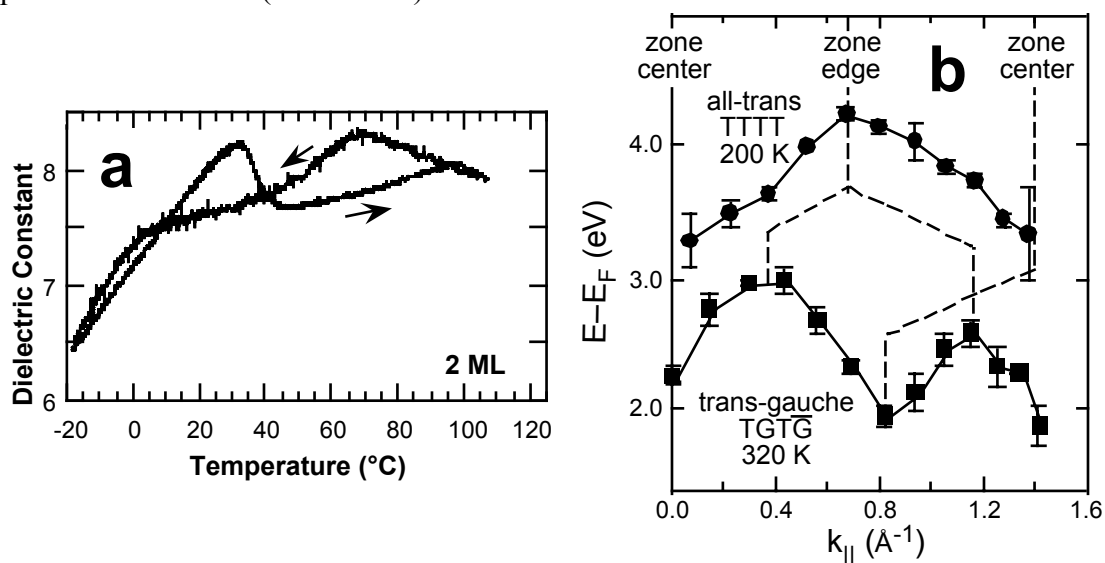


FIGURE 8. Evidence for the surface phase transition in P(VDF-TrFE 70:30 LB films. a) The dielectric response of a 2-ML film (Reprinted by permission from Nature, Ref. 12, © 1998 Macmillan Magazines Ltd.); b) The doubling of the surface Brillouin zone due to conversion of the polymer chain configuration from all-trans ($TTTT$) to alternating trans-gauche ($TGT\bar{G}$). (Adapted from Ref. 9.)

EXTRINSIC PROPERTIES

Pyroelectric and Piezoelectric Response

Detailed measurements of the pyroelectric response (charge generated on heating or cooling) and piezoelectric response (strain in an electric field) confirm with unprecedented detail that both properties are directly proportional to the spontaneous polarization, a basic result predicted by ferroelectric theory. Both properties exhibit hysteresis on voltage cycling (Fig. 9a) and the proportionality between the two responses is demonstrated in Fig. 9b.²⁴

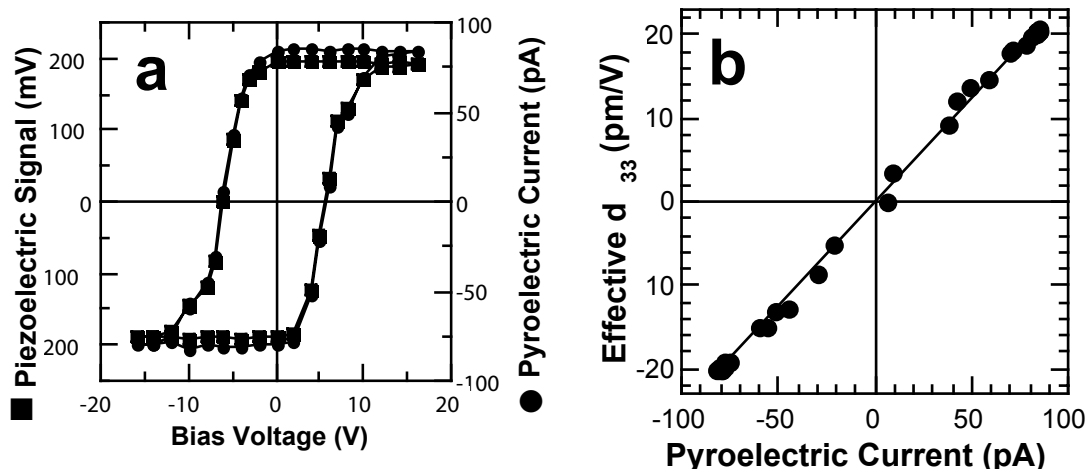


FIGURE 9. Piezoelectric and Pyroelectric responses in a 30-ML film of P(VDF-TrFE 70:30). (Adapted from Ref. 24.) a) Hysteresis of the piezoelectric and pyroelectric responses as the electric field is cycled around the polarization hysteresis loop; b) Demonstration of the linear relation between the piezoelectric and pyroelectric responses.

We have imaged the spatial distribution of polarization in the films by Scanning Pyroelectric Microscopy (SPM), measurement of the pyroelectric current due to heating by a focused laser beam scanned across the film. The SPM technique allows us to probe crystallite and domain structure with fine spatial and temporal resolution.

Switching Dynamics

One of the more puzzling results of our studies over the last five years is that many of the LB films have very slow switching (polarization reversal), taking 10-100 seconds, a serious impediment to applications of these films to, e.g., nonvolatile data storage. The switching rate may be low because nucleation is suppressed by the two-dimensionality of the films. But we have found that the LB films can be made to switch much faster, in 1-5 μ s, and are presently investigating the causes.

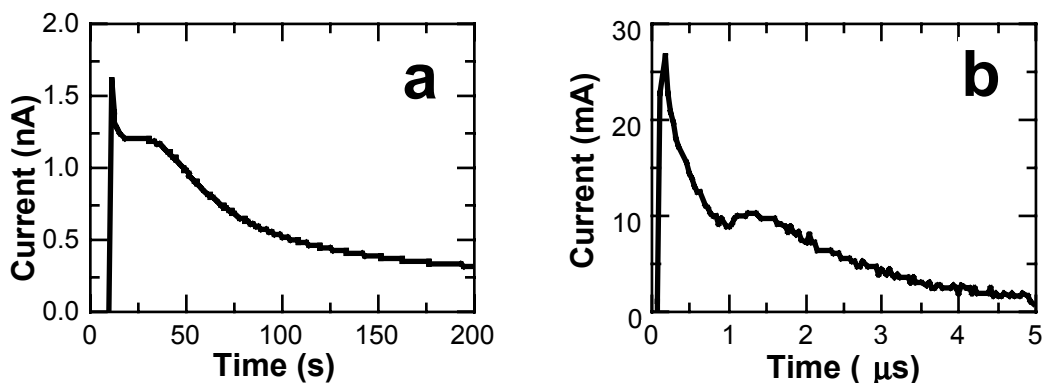


FIGURE 10. Switching transients: a) in a 30-ML film on glass; b) in a 8-ML film on Si.

Potentially Useful Applications

The parent polymer poly(vinylidene fluoride) has been in wide use for nearly 20 years in piezoelectric transducers for electromechanical actuators, soft-touch switches, strain gauges, and in sonar and ultrasound transducers. The LB polymer films have large pyroelectric response²⁴ over a useful range $-50\text{ }^{\circ}\text{C}$ to $100\text{ }^{\circ}\text{C}$, making them candidate infrared sensors for low-cost uncooled infrared imaging systems. The films exhibit a novel 1000:1 conductance switching when the film polarization is reversed and this might be exploited in nonvolatile random access data storage with non-destructive readout.²⁵

One of the surprising results of this work is the electrical robustness of the films. They hold off electric fields over 3 GV/m (3 *billion* volts per meter), more than any other material reported to date, and approaching the ionization potential of the valence electrons! This is possible because the high quality films at least 2 ML thick lack electrical shorts, and since this field strength is achieved with only a few volts applied, avalanche breakdown is avoided. Since the energy density of a capacitor is proportional to the dielectric constant divided by the square of its thickness, decreasing the thickness is more effective than increasing the dielectric constant. These nm-thick films, even with a low dielectric constant of only $\kappa \approx 8$, have achieved record high energy density of over 400 Joules per cubic centimeter. A multilayer capacitor made from these films this could revolutionize portable power, lightening many mechanical and electronic devices that use heavy capacitors or batteries. As an added bonus, capacitors, unlike batteries, will work well in the cold Nebraska and Moscow winters.

The main advantages of ferroelectric polymers are the low production costs, ease and flexibility (literally and figuratively) of fabrication in a variety of thin film forms, and resistance to degradation caused by strain. Polymers are more readily altered to conform to complex device requirements imposed by the environment, size, shape, physical flexibility, reliability, durability, and other constraints. Films can be readily patterned for integrated electronic applications. Ferroelectric polymer films need not be grown epitaxially, a difficult constraint for many other ferroelectric films, yet they adhere well to a wide variety of substrates. The main disadvantages of polymers are their chemical, thermal and mechanical vulnerability.

ACKNOWLEDGMENTS

Work at the University of Nebraska was supported by the USA National Science Foundation, the USA Office of Naval Research, the USA Air Force Office of Scientific Research, and the Nebraska Research Initiative through the Center for Materials Research and Analysis. Work at the Institute of Crystallography was supported by the Russian Foundation for Basic Research (#99-02-16484) and the Inco-Copernicus programme (#IC15-CT96-0744).

REFERENCES

1. A. J. Lovinger, *Macromol.* **16**, 1529 (1983).
2. T. Furukawa, *Phase Transitions* **18**, 143 (1989).
3. K. Tashiro, in *Ferroelectric Polymers*, H. S. Nalwa ed. (Marcel Dekker, New York, 1995), pp. 63.
4. T. T. Wang, J. M. Herbert, A. M. Glass, eds., *The Applications of Ferroelectric Polymers*, (Chapman and Hall, New York, 1988).
5. J. K. Krüger, B. Heydt, C. Fischer, J. Baller, R. Jiménez, K.-P. Bohn, B. Servet, P. Galtier, M. Pavel, B. Ploss, M. Beghi, C. Bottani, *Phys. Rev. B* **55**, 3497 (1997).
6. K. Omote, H. Ohigashi, K. Koga, *J. Appl. Phys.* **81**, 2760 (1997).
7. S. Palto, L. Blinov, A. Bune, E. Dubovik, V. Fridkin, N. Petukhova, K. Verkhovskaya, S. Yudin, *Ferro. Lett.* **19**, 65 (1995).
8. A. V. Sorokin, "Langmuir-Blodgett Deposition of Ferroelectric Polymer Films," Ph.D. Dissertation, (Institute of Crystallography, 1997).
9. J. Choi, P. A. Dowben, A. V. Bune, S. Ducharme, V. M. Fridkin, S. P. Palto, N. Petukhova, *Phys. Lett. A* **249**, 505 (1999).
10. J. Choi, C. N. Borca, P. A. Dowben, A. V. Bune, M. Poulsen, S. Pebley, S. Adenwalla, L. Robertson, S. Ducharme, V. M. Fridkin, S. P. Palto, N. Petukhova, S. G. Yudin, *Phys. Rev. B* to appear in (2000).
11. C. N. Borca, J. Choi, S. Adenwalla, S. Ducharme, P. A. Dowben, L. Robertson, V. M. Fridkin, S. P. Palto, N. Petukhova, *Appl. Phys. Lett.* **74**, 347 (1999).
12. A. V. Bune, V. M. Fridkin, S. Ducharme, L. M. Blinov, S. P. Palto, A. Sorokin, S. G. Yudin, A. Zlatkin, *Nature* **391**, 874 (1998).
13. J. Choi, P. A. Dowben, S. Pebley, A. V. Bune, S. Ducharme, V. M. Fridkin, S. P. Palto, N. Petukhova, *Phys. Rev. Lett.* **80**, 1328 (1998).
14. S. Ducharme, A. V. Bune, V. M. Fridkin, L. M. Blinov, S. P. Palto, A. V. Sorokin, S. Yudin, *Phys. Rev. B* **57**, 25 (1998).
15. S. Ducharme, V. M. Fridkin, A. Bune, S. P. Palto, L. M. Blinov, N. N. Petukhova, S. G. Yudin, *Phys. Rev. Lett.* **84**, 175 (2000).
16. L. M. Blinov, V. M. Fridkin, S. P. Palto, A. V. Bune, P. A. Dowben, S. Ducharme, *Physica Uspekhi* (1999).
17. D. R. Tilley, in *Ferroelectric Thin Films: Synthesis and Basic Properties*, C. Paz de Araujo, J. F. Scott, and G. F. Taylor eds., (Gordon and Breach, Amsterdam, 1996), pp. 11.
18. K. Dimmler, M. Parris, D. Butler, S. Eaton, B. Pouligny, J. F. Scott, Y. Ishibashi, *J. Appl. Phys.* **61**, 5467 (1987).
19. J. F. Scott, M. S. Zheng, R. B. Godfrey, C. A. Paz de Araujo, L. D. McMillan, *Phys. Rev. B* **35**, 4144 (1987).
20. K. Ishikawa, K. Yoshikawa, N. Okada, *Phys. Rev. B* **37**, 5852 (1988).
21. K. Kimura and H. Ohigashi, *Jpn. J. Appl. Phys.* **25**, 383 (1986).
22. L. M. Blinov, V. M. Fridkin, S. P. Palto, A. V. Sorokin, S. G. Yudin, *Thin Solid Films* **284-85**, 474 (1996).
23. O. A. Aktsipetrov, T. V. Misuryaev, T. V. Murzina, *Opt. Lett.* **March**, (2000).
24. A. V. Bune, C. Zhu, S. Ducharme, L. M. Blinov, V. M. Fridkin, L. Blinov, S. Palto, N. G. Petukhova, S. G. Yudin, *J. Appl. Phys.* **85**, 7869 (1999).
25. A. Bune, S. Ducharme, V. M. Fridkin, L. Blinov, S. Palto, N. Petukhova, S. Yudin, *Appl. Phys. Lett.* **67**, 3975 (1995).